The Astrophysical Journal, 941:94 (8pp), 2022 December 10 https://doi.org/10.3847/1538-4357/ac9d3a

Radiation-induced D-to-H Exchange in Ices Containing Ethane or Benzene: Reactions and Rate Constants

Christopher K. Materese
Astrochemistry Laboratory, NASA Goddard Space Flight Center, Greenbelt, MD 20771, USA; Christopher.K.Materese@nasa.gov
Received 2022 June 17; revised 2022 October 18; accepted 2022 October 22; published 2022 December 14

Abstract

The rate constants for radiation-induced deuterium to hydrogen (D-to-H) exchange were recently measured for CD_4 in H_2O and C_2D_6 in H_2O at 20 K. In the current study, rate constants for radiation-induced D-to-H exchange were obtained for C_6D_6 in H_2O at 20, 50, and 100 K. The rate constants for D-to-H exchange for an organic molecule in water were found to be an order of magnitude greater for benzene than ethane. Additionally, D-to-H exchange for benzene was found to be far more favorable than the production of any other radiolysis product, a result that contrasts with our previous findings for methane and ethane. Finally, rate constants were obtained for C_2D_6 in H_2O at 50 K. For all ice mixtures, increasing the temperature of the experiment yielded a larger rate constant. There is a notable difference in the magnitude of the response of the rate constant for D-to-H exchange as a function of temperature for C_2D_6 versus C_6D_6 containing ices. The results suggest that radiation will have an asymmetric effect on D-to-H exchange between different types of organic compounds and water ice matrices. These results suggest that the radiation history of an extraterrestrial sample will influence the D/H ratios of its organic compounds.

Unified Astronomy Thesaurus concepts: Astrochemistry (75); Reaction rates (2081)

1. Introduction

Organic compounds of interstellar origin typically possess elevated deuterium (D)/hydrogen (H) ratios compared to those in most compounds across the solar system today. Much of this enhanced deuterium fractionation is believed to be a consequence of low-temperature, gas-phase ion-molecule reactions (Watson 1976, 1977; Snyder et al. 1977; Geiss & Reeves 1981; Dalgarno & Lepp 1984). Specifically, the enrichment is caused by differences in zero-point vibrational energies in the reaction $H_3^+ + HD \rightleftharpoons H_2D^+ + H_2$ (Watson 1976; Snyder et al. 1977). As temperatures approach absolute zero, the forward reaction is increasingly favored (Smith et al. 1982; Herbst 1982), leading to a relatively high abundance of H_2D^+. The H_2D^+ can then participate in the synthesis of simple organic compounds such as HCN/DCN and HCO/DCO, which in turn can form larger organic compounds with enhanced deuterium fractionation. Additionally, low-temperature gas–grain chemistry is also a possible source of deuterium enrichment in cold interstellar clouds (Tielens 1983).

During the formation of the solar system, organic compounds of interstellar origin might have condensed onto dust grains along with water and other inorganic compounds. Over time, these icy grains might have been incorporated into larger bodies, which serve as repositories of primitive organic materials and can preserve enhanced deuterium fractionation. Consequently, the D/H ratio is considered a useful tracer for determining the processes involved in the origin and formation of compounds in extraterrestrial samples (Robert & Epstein 1982; Yang & Epstein 1983; Kerridge & Chang 1985; Krishnamurthy et al. 1992).

Once incorporated into larger bodies, the D/H ratio of organic compounds can be modified by different processes. Importantly, interstellar organics tend to have significantly higher D/H ratios than water (Cleeves et al. 2016) meaning reactions with water will erode the enhanced fractionation of these organics. For example, parent body aqueous chemistry will readily result in the exchange of D and H between water and any functional groups (e.g., amines, hydroxyl) of an organic compound containing labile hydrogen without otherwise altering that compound (Faure et al. 2015).

Surface processes have also been shown to result in H/D exchange for some protiated organic compounds that are exposed to deuterium atoms and some deuterated organic compounds exposed to H atoms. For example, Watanabe & Kouchi (2008) demonstrated that H-to-D and D-to-H substitutions can occur in formaldehyde; however only the H-to-D substitution was observed in methanol. In that study it was not clear if the exchange reaction in formaldehyde occurred via a succession of abstraction followed by addition, or if a direct exchange occured. In contrast the authors concluded that for methanol the exchange likely occurred via a succession of tunneling H abstraction followed by D addition. Similar experiments attempting to study H-to-D exchange in ethane exposed to deuterium beams were conducted by Hiraoka et al. (2000) and later by Kobayashi et al. (2017). In the former paper, H-to-D exchange for ethane was below the detection limit for temperatures above 20 K and was not observed at all in the latter paper. It was also shown that the H and D atom abstractions from hydrocarbons by OH radicals can lead to H-to-D exchange through the surface processes (Lamberts et al. 2017).

Radiation- or photo-induced D-to-H exchange in organic molecules embedded in water ice may also play an important role in their current D/H ratios (Sandford et al. 2000, 2001; Qasim et al. 2022). Icy bodies are subjected to radiation in the forms of solar wind particles, magnetospheric radiation,

galactic cosmic rays, and electromagnetic radiation. Laboratory studies demonstrated that UV photolysis readily induces H-to-D exchange for coronene in a D_2O matrix and D-to-H exchange for perdeuterated coronene in H_2O (Sandford et al. 2000). More recently, rate constants were obtained for radiation-induced D-to-H and H-to-D exchange between small aliphatic compounds (methane and ethane) and water (Qasim et al. 2022). In those experiments, ices consisting of CD_4 or C_2D_6 mixed with H_2O (1:50 ratio) were irradiated with 0.9 MeV protons. The experiments were repeated with CH_4 and C_2H_6 in D_2O (1:50 ratio). The radiolytic depletion of the reactant hydrocarbon and the formation of its singly deuterated or protiated isotopologue was monitored using infrared (IR) spectroscopy. The rate constants for a single D-to-H exchange were found to be nearly identical for CD_4 and C_2D_6 in H_2O and were *lower* than the rate constants for H-to-D exchange for CH_4 or C_2H_6 in D_2O. Notably, rate constants for H-to-D exchange were determined to be nearly the same as the rate constants for the formation of *all other* possible radiolysis products combined. For D-to-H exchange, the rate constants were roughly half those for the formation of all other products combined.

Our previous work suggests that radiation-induced D-to-H exchange might have an impact on analyses of extraterrestrial samples that use D/H ratios to determine if a compound detected in a meteorite or other sample originated in the interstellar medium (ISM). This exchange process could result in a variation in D/H ratios for organic compounds produced in the ISM as a function of depth from the surface of an large icy body. Specifically, organic compounds originating in the ISM that are closer to the surface of these bodies and receive the largest radiation doses will experience a greater suppression of their D/H ratios than those found at a greater depth.

This Paper will focus on solid-phase radiation-induced D-to-H exchange in perdeuterated ethane (C_2D_6) and the influence of temperature on the rate constants. Additionally, similar experiments were performed using perdeuterated benzene (C_6D_6), to compare the rate constants of D-to-H exchange in a relatively small aromatic compound to our previous results for small aliphatic compounds. These molecules were selected as simple representatives of their molecular classes because a single D-to-H exchange will always yield a single isotopologue, greatly simplifying the analysis.

It is important to note that fully deuterated compounds are not expected to be the dominant form of these compounds in space. Further I must emphasize that the rate constants for D-to-H exchange for molecules that are not fully deuterated will differ from those discussed in this Paper because of statistical and energetic factors. Using C_6D_6 as an example, H from the water can only exchange with D to yield C_6D_5H. In contrast, for C_6H_5D, H from water could exchange with the one D atom or trivially exchange with one of the other 5 H atoms already present. Further complicating matters, the C–H bond is more easily broken than the C–D bond meaning the trivial H-to-H exchange becomes even more likely. Because of this, these rate constants should not be directly applied to the analysis of extraterrestrial compounds, but instead should be used as a guide to understand the processes occurring. In other words, this work could be considered a first-order approximation of the importance of radiolytic D/H exchange and can be used understand the relative impact of this process for different types of molecules (aliphatic versus aromatic), at different ice temperatures.

2. Experimental Methods

The current experiments used the methods outlined in Qasim et al. (2022). Briefly, all experiments were conducted in a high-vacuum chamber ($\sim$1–2 $\times$ 10^{-7} torr when cooled, $\sim$7–8 $\times$ 10^{-7} at room temperature) equipped with a cryocooler. This chamber, thoroughly described in Hudson & Ferrante (2020), was interfaced with a Van de Graaff accelerator capable of irradiating an ice sample with 0.9 MeV p^+. The chamber was also interfaced with a Nicolet iS50 infrared spectrometer (5500–500 cm^{-1} spectral range, 256 scans, 4 cm^{-1} resolution, transmission mode, with a DTGS detector), which was used to monitor and quantify the radiolysis.

Amorphous ice films were generated via vapor deposition onto a KBr substrate at 20 K and growth rates were monitored using interference fringes from a 670 nm laser. The relative abundances of the reactant water and organic molecules were set by leak valves that were calibrated for each compound. Ice mixtures of 1:50 perdeuterated organic molecules: H_2O were generated for all experiments presented in this Paper. For all experiments, the ices were grown to a thickness of 3 μm, significantly less than the penetration depth of 0.9 MeV protons ($\sim$25 μm). Following the deposition, if the radiolysis was planned for a temperature other than 20 K then samples were heated to the required temperature at a rate of 2 K $minute^{-1}$. Ices are assumed to be homogeneous mixtures upon deposition and remain so throughout the experiment.

Target infrared bands for C_2D_6 (with C_2D_5H) and C_6D_6 (with C_6D_5H) were chosen by examining the IR spectra of each compound in a 1:50 organic:H_2O ice and selecting the bands that were minimally obscured by the solvent and had minimal obvious overlap with other known bands of interest when possible (this was not avoidable for the reactants). Reference intrinsic band strengths for C_2D_6 and C_2D_5H were collected in Qasim et al. (2022) and are used in this work (Table 1). Intrinsic band strengths for C_6D_6 and C_6D_5H were obtained (Table 1) using the same technique. These intrinsic band strengths were used to quantify the column densities of the reactants and singly protiated products during each experiment. Control experiments were performed to verify that these intrinsic band strengths do not change as a function of ice thickness and no significant variation with temperature was observed over the ranges examined during this study. Although it is not feasible to test whether changes in the ice morphology because of p^+ bombardment could alter these band strengths, please note that radiation exposure tends to amorphize an ice and since the ice is already amorphous, any potential effects should be minimized. The measurable fully deuterated reactant bands all at least partially overlapped with those of the singly protiated product, making it essential to account for this when computing the reactant column densities after the radiolysis had begun.

Once the ice was deposited but prior to irradiation, an IR spectrum was collected and target bands (Table 1) were integrated to obtain the initial column densities of the reactants and products. Note that the initial column density of the "product" should not be presumed to be zero because the reactant organics possessed some contaminant hydrogen (e.g., the C_2D_6 contained some C_2D_5H). The ice was then exposed to 0.9 MeV p^+ radiation at a current of 50 nA and after a prescribed absorbed dose, a new IR spectrum was collected.

Table 1
Physical Properties and Selected Band Strengths of Reactants and Products

Molecule (Brand and Purity)	n[e] (670 nm)	ρ[e] (gcm^{-3})	Band (cm^{-1})	Approximate Description	A[f] (cm $molecule^{-1}$)
C_2D_6 (MSD Isotopes 99.8%)	1.31[a]	0.86[a]	1071	CD_3 deformation[c]	1.34×10^{-18}
C_2D_5H (Cambridge isotope lab D5-98%)	1.31[a]	0.84[a]	1068 1301	CD_3 deformation[c] CD2H deformation[c]	8.91×10^{-19} 8.54×10^{-19}
C_6D_6 (Sigma-Aldrich 99%)	1.402[b]	0.828[b]	1330[d]	CC/CX stretch[d]	1.90×10^{-18}
C_6D_5H (Sigma-Aldrich D5-99%)	1.402[b]	0.818[b]	1387[d] 1341[d]	CC stretch[d] CX stretch[d]	9.35×10^{-19} 9.69×10^{-19}

Notes. Products have two bands listed because of bands that overlap with the target reactant band that must be accounted for.
[a] Values from Satorre et al. (2017).
[b] Values from Hudson & Yarnall (2022).
[c] Benedict et al. (1937); Stitt (1939); Pinchas & Laulicht (1971).
[d] Nanney et al. (1966).
[e] n was obtained for protiated species and ρ was determined by scaling the densities of protiated species by the ratio ($m_{\text{D-isotopologue}}/m_{\text{fully protiated}}$).
[f] In a 1:25 organic:water ice (for C_2D_6) or in a 1:50 organic:water ice (for C_6D_6).

The ice's stopping power, and from it the absorbed dose, was determined using the stopping and eange of ions in matter (SRIM) software (Ziegler et al. 2010). From there, the cycle of irradiation of the sample followed by collection of an IR spectrum was repeated until the end of the experiment. To provide some additional context for the radiation doses used in these experiments, a table of annual radiation doses in various space environments has been included (Table 2).

Please note that while it should be possible to study D-to-H exchange for C_2H_5D in H_2O (yielding C_6H_6 as the protiated product) it would not be practical to use these experimental techniques to study C_6H_5D in H_2O. Specifically, to follow the formation of C_6H_6 in the infrared, it would be necessary to measure the increase in absorbance of IR features that overlap with reactant bands or conflict strongly with solvent bands. This is not feasible because the reactants are being simultaneously consumed and converted into other products (aside from the fully protiated product), meaning that any increase in band strength associated with the protiated product will be simultaneously obscured by loss of band strength from the consumption of the reactant. Because of this limitation, this Paper will only examine D-to-H exchange in fully deuterated species so that a straightforward comparison can be made between the results of the C_2D_6 and C_6D_6 experiments.

3. Results

As in Qasim et al. (2022), the D-to-H exchange kinetics were treated as a system of parallel irreversible first-order reactions (1a) and (1b):

$$A \xrightarrow{k_1} B \tag{1a}$$

$$A \xrightarrow{k_2} P \tag{1b}$$

where A is the perdeuterated reactant compound, B is the singly protiated product, P represents any other products made from A, and k_1 and k_2 are the rate constants of the respective reactions (MGy^{-1}). The irreversibility of the reactions and the nonconsideration of any subsequent reactions (i.e., $B \rightarrow$ something else) makes this a somewhat simplified reaction scheme, but reasonable when considering that experiments are terminated before a majority of the reactants are consumed. To determine the rate constants, the integrated rate Equations (2) and (3) were simultaneously fit to the destruction and formation data from the IR spectra by using a nonlinear least-squares algorithm.

Table 2
Estimated Annual Radiation Doses in Space Environments

Location	T (K)	Depth (cm)	Dose Rate (Gy yr^{-1})
Europa[a]	100	10^{-3}	$18. \times 10^{7}$
		1	1.2×10^{4}
		100	1.7×10^{0}
Comets[b]	40	10^{-4}	5.4×10^{0}
		1	4.1×10^{-2}
Diffuse[c] ISM	40	⋯	5.4×10^{5}
Dense[c] ISM	10	⋯	1.1×10^{2}

Notes. Original data sources:
[a] Paranicas et al. (2009); dose rate includes protons and electrons.
[b] Strazzulla et al. (2003).
[c] Moore et al. (2001); dose includes protons and UV photons.

$$\frac{[A]}{[A]_0} = e^{-(k_1+k_2)D} \tag{2}$$

$$\frac{[B]}{[A]_0} = \frac{k_1}{(k_1+k_2)}(1 - e^{-(k_1+k_2)D}) + c \tag{3}$$

In Equations (2) and (3), [A] and [B] are the reactant and product column densities, respectively, $[A]_0$ is the initial column density, and c is related to the presence of contaminant hydrogen in the reactant organic. The rate constants k_1 and k_2 and c were extracted from the curve fitting.

Figure 1 shows the IR spectra of both C_2D_6 in H_2O (1:50) and C_6D_6 in H_2O (1:50) at 20 K collected during a typical radiolysis experiment. The spectra of the C_6D_6 in H_2O ice have a residual D_2O/HDO contamination of approximately 2% (as determined by band areas) relative to H_2O from prior experiments involving pure D_2O. The spectra shown represent the worst level of D_2O/HDO contamination in any of these experiments, and at these levels do not significantly impact the results. Since the features of interest are very small, these spectra are only shown for reference, and the radiolysis results that follow focus on target infrared bands.

Figure 2 shows expansions of the IR spectra of both C_2D_6 in H_2O (1:50) and C_6D_6 in H_2O (1:50) at 20 K collected during a typical radiolysis experiment. As the radiolysis progresses, the bands corresponding to C_2D_6 and C_6D_6 both decrease with an increasing dose while bands corresponding to their respective

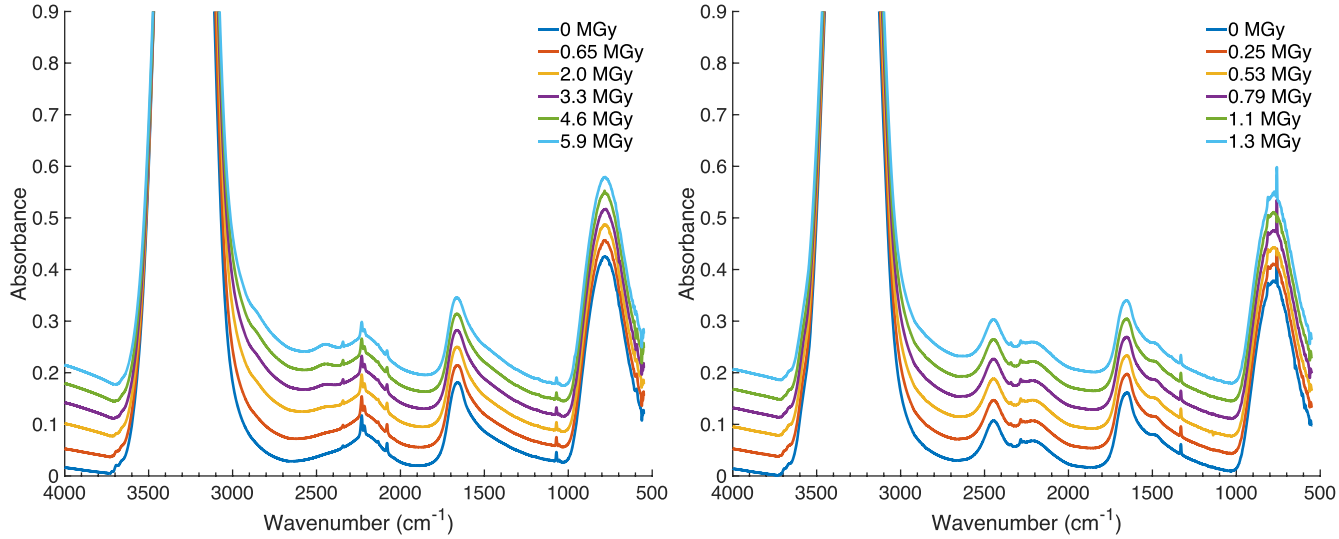

Figure 1. IR spectra of $C_2D_6 + H_2O$ (left) and $C_6D_6 + H_2O$ (right) 1:50 mixtures at 20 K before and after radiolysis. Please note there is ∼2% D_2O/HDO contamination in the C_6D_6 + H2O mixture.

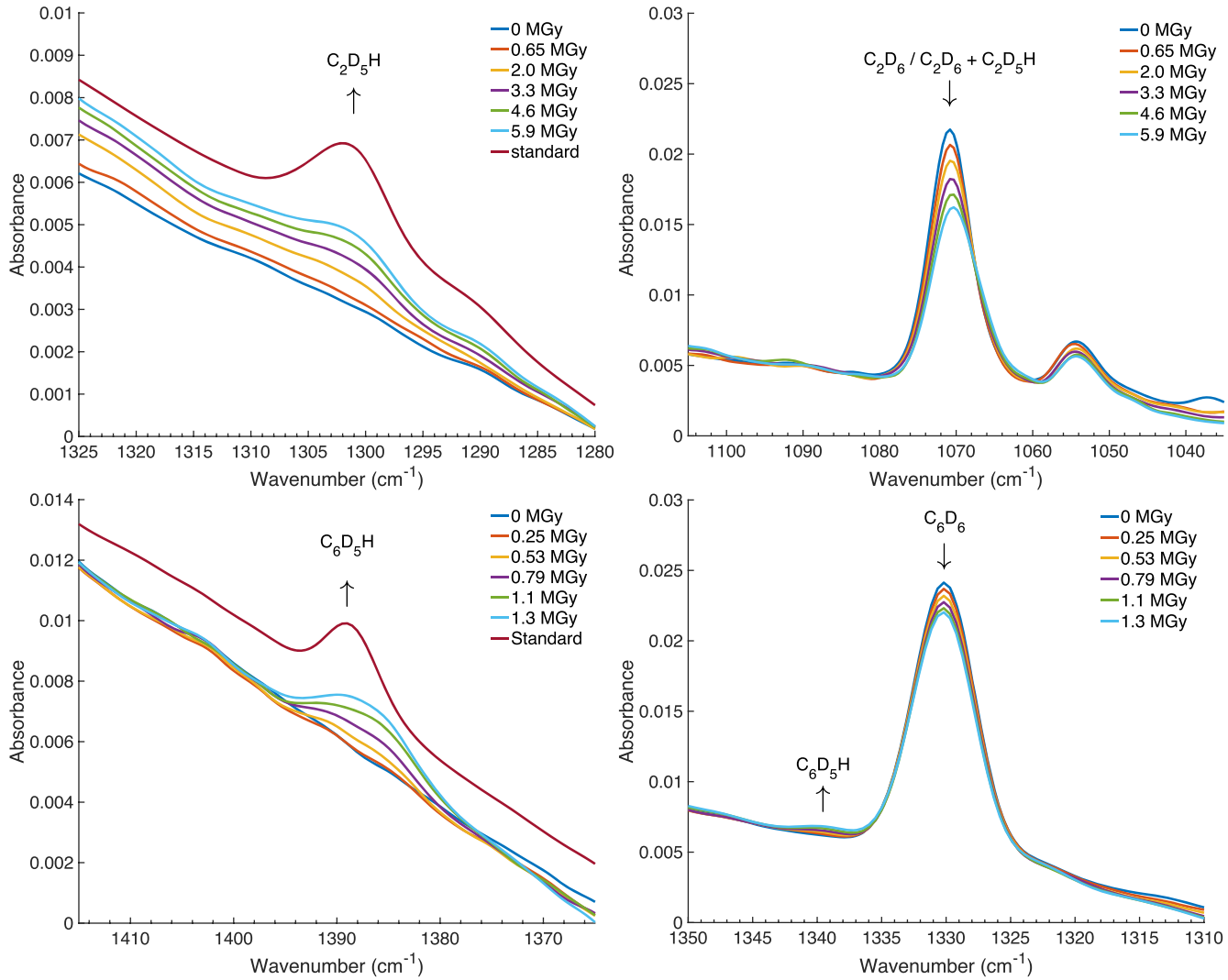

Figure 2. The IR spectra of $C_2D_6 + H_2O$ [1:25] (top) and $C_6D_6 + H_2O$ [1:50] (bottom) mixtures at 20 K before and after exposure to radiation (data originally in Qasim et al. 2022). Arrows identify peaks and indicate the direction of increasing dose. Note that after irradiation, the bands marked as C_2D_6 and C_6D_6 cannot be exclusively attributed to these molecules and also contain some contribution from C_2D_5H and C_6D_5H, respectively. The spectra tracking the growth of C_2D_5H and C_6D_5H also include reference spectra from their commercial standards in H_2O to demonstrate the expected band positions for these molecules. Please note, the spectra of the standards have been scaled down (by a factor of 5) and baseline adjusted for easier comparison with the experimental data.

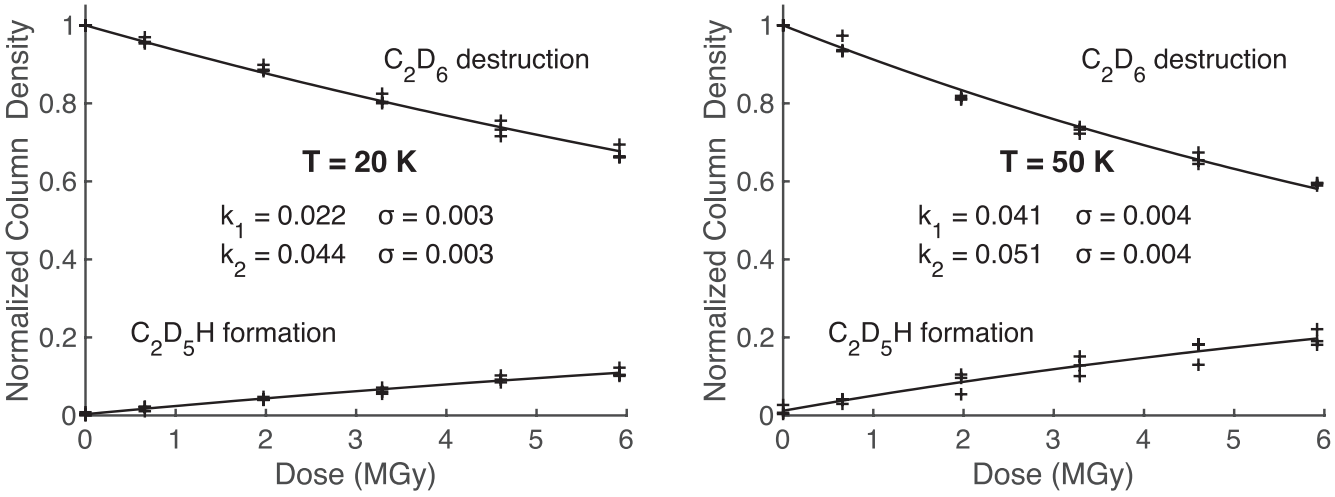

Figure 3. Data showing the loss of C_2D_6 and the simultaneous growth of C_2D_5H at 20 K (*left*) and 50 K (*right*). Equations (2) and (3) were fit to the destruction and formation data, respectively, and the corresponding best-fit curves are included in the figures. The column densities for reactants and products are normalized to the maximum column density of the reactant (~2.1 (±0.2) × 10^{17} molecules cm^{-2}). Each experiment was performed in triplicate and the average rate constants k_1 and k_2 along with their standard deviations are shown.

Table 3
Kinetic Parameters for the Radiolysis of Perdeuterated Ethane and Benzene in H_2O at 20, 50, and 100 K

Ice Mixture (1:50)	Protiated Product	k_1 (MGy^{-1})	k_2 (MGy^{-1})	c
$C_2D_6 + H_2O$ (20 K)[a]	C_2D_5H	0.022 ± 0.003	0.044 ± 0.003	0.003 ± 0.002
$C_2D_6 + H_2O$ (50 K)	C_2D_5H	0.041 ± 0.004	0.051 ± 0.004	0.012 ± 0.010
$C_6D_6 + H_2O$ (20 K)	C_6D_5H	0.150 ± 0.015	0.001 ± 0.001	0.020 ± 0.011
$C_6D_6 + H_2O$ (50 K)	C_6D_5H	0.180 ± 0.044	<0.001 ± <0.001	0.057 ± 0.016
$C_6D_6 + H_2O$ (100 K)	C_6D_5H	0.240 ± 0.020	0.002 ± 0.004	0.054 ± 0.021

Note.
[a] $C_2D_6 + H_2O$ (20 K) data are taken from Qasim et al. (2022).

singly protiated isotopologues grow. Note that after the radiolysis has begun, the band corresponding to C_2D_6 no longer uniquely belongs to this compound, but now overlaps with a band of C_2D_5H (see Table 1), and consequently the band's area must be adjusted by subtracting the product contribution to account for this overlap. The same issue of an overlapping reactant and product bands partially occurs for the 1330 cm^{-1} band associated with C_6D_6 and the 1341 cm^{-1} band associated C_6D_5H and is similarly accounted for. While not quantitatively useful, the 1341 cm^{-1} band provides further qualitative confirmation of the formation of C_6D_5H as it is clearly shown to grow with increasing radiation dose (Figure 2).

Figure 3 shows the data for the radiolytic destruction of C_2D_6 and formation of C_2H_5D at 20 K (left) and 50 K (right) along with their corresponding best-fit curves (fitting parameters are in Table 3). The column densities of all reactants and products are normalized to the initial column density of the reactant as shown in Equations (2) and (3). Each experiment was performed three times and the average of the rate constants are reported along with their standard deviations (σ). These data demonstrate that increasing the temperature from 20 to 50 K has a dramatic effect of nearly doubling the rate constants k_1 for D-to-H exchange. In contrast, this temperature increase only results in a modest ~10% increase in the rate constant k_2 for the formation of all other products.

Figure 4 shows the data for the radiolytic destruction of C_6D_6 and formation of C_6H_5D at 20 K (top), 50 K (middle), and 100 K (bottom) along with their corresponding best-fit curves (fitting parameters are shown in Table 3). The rate constants k_1 obtained for the conversion of C_6D_6 to C_6D_5H are an order of magnitude higher than those for the conversion of C_2D_6 to C_2D_5H. Interestingly, unlike the experiments involving ethane, k_2 for the benzene experiments is dramatically smaller than k_1 suggesting that nearly all of the depletion of C_6D_6 is due to the formation of C_6D_5H. These data demonstrate that the rate constant k_1 increases when the temperature is raised from 20 to 50 or 100 K (Figure 5) while no measurable change in k_2 is observed. Notably, the temperature dependent increase in k_1 for C_6D_5H formation from C_6D_6 is far more modest than is observed for C_2D_5H from C_2D_6 with only a 20% increase from 20 to 50 K and only a 60% increase from 20 to 100 K. The dramatic difference in the relative magnitude of the rate constants k_1 and k_2 for the radiolysis of perdeuterated ethane in water versus perdeuterated benzene in water, in addition to the difference in these rate constants as a function of temperature, suggests D-to-H exchange may be governed by different reaction mechanisms.

Radiation-free control experiments were also performed for both C_2D_6 in H_2O (at 50 K) and C_6D_6 in H_2O ice mixtures (at 100 K). In these experiments, ice mixtures were deposited at 20 K and heated to 50 or 100 K (for C_6D_6 only) where they were held for ~20 hr and no evidence of D-to-H exchange was observed for either mixture demonstrating that the exchange is not spontaneous.

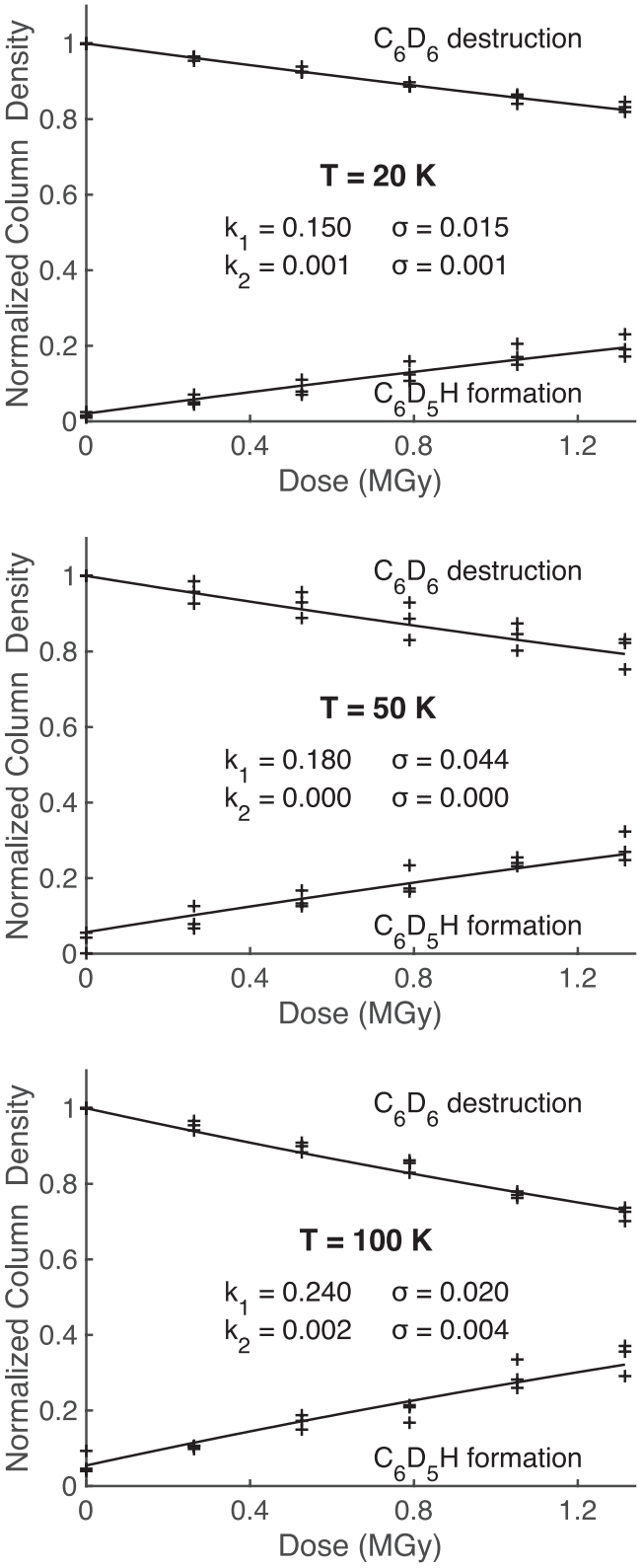

Figure 4. Data showing the loss of C_6D_6 and the simultaneous growth of C_6D5_H at 20 K (top), 50 K (middle), and 100 K (bottom). Equations (2) and (3) were fit to the destruction and formation data, respectively, and the corresponding best-fit curves are included in the figures. The column densities, for reactants and products are normalized to the maximum column density of the reactant (~1.5 (±0.1) × 10^{17} molecules cm^{-2}). Each experiment was performed in triplicate and the average rate constants k_1 and k_2 along with their standard deviations are shown.

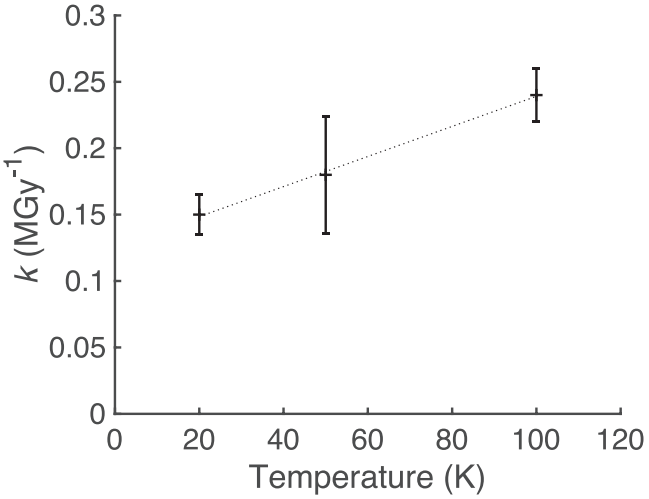

Figure 5. The rate constants k_1 at 20, 50, and 100 K.

4. Discussion

The previous studies involving D/H exchange (Hiraoka et al. 2000; Kobayashi et al. 2017) indicate that nonthermal processes play a critical role in the D-to-H exchange reactions for solid C_2D_6 with H_2O in the present study and in Qasim et al. (2022). In our previous paper (Qasim et al. 2022) we suggested that the D-to-H exchange in CD_4 and C_2D_6 may have proceeded primarily through ions and radicals originating in the water reacting with closed-shell organic species. Our proposed mechanism involved a three-step process where (1) reactive species are produced in the ice, (2) a D atom is abstracted from the organic compound leaving an ion or energetic radical intermediate, (3) the unstable intermediate combines with a hydrogen from the surrounding ice. In our first paper, we attributed differences in the rate constants between methane and ethane and their respective isotopologues as being mostly controlled by differences in relative bond dissociation energies. In the present experiments, the 20 K rate constant for D-to-H exchange in benzene is an order of magnitude greater than those measured for methane and ethane at the same temperature. Additionally, the rate constant k_2 for the C_6D_6 experiments are nearly zero while they exceed k_1 for C_2D_6. Subtle differences in bond dissociation energies alone cannot explain these stark differences.

Previous studies involving the bombardment of benzene with D atoms resulted in deuteration via reduction of benzene (addition of deuterium atoms and elimination of double bonds) rather than H-to-D exchange (Hama et al. 2015). In contrast, these radiolysis experiments show that for nearly every C_6D_6 molecule consumed, a C_6D_5H is created. This further suggests that nonthermal energetic processes play a vital role in D-to-H exchange.

The D-to-H exchange rate in benzene may be controlled by the addition of energetic H atoms and H^+ ions to C_6D_6, followed by the ejection of a D ion or radical. This reaction scheme (Equations (4a), (4b)) might proceed much more rapidly and result in far less conversion of the benzene to other potential products because of the mobility and high affinity of the reactive H^- and H^+ for the electrons in the π-systems on benzene and because of the relative stability of the intermediate aromatic species.

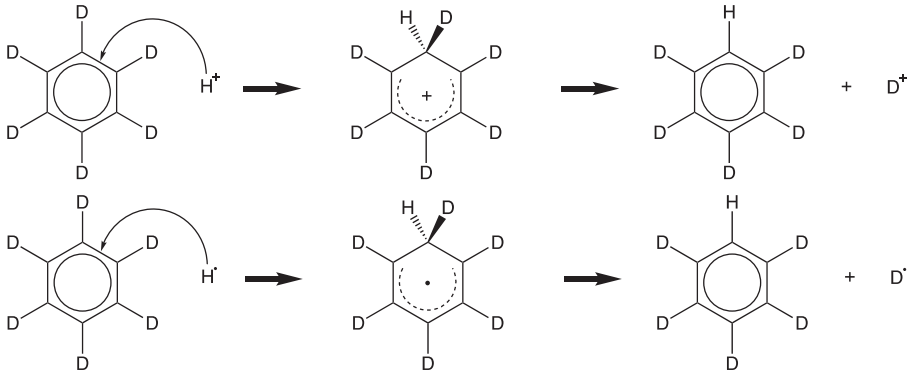

This work also provides further insight into why, in our first paper, we were unable to observe D/H exchange between ethylene and water or acetylene and water. Like benzene, ethylene and acetylene possess π-orbitals that would be highly reactive with mobile $H^{\cdot}$ and H^{+}. Unlike benzene, after the initial addition of $H^{\cdot}$ or H^{+}, the resulting intermediate would not be as stable and would likely undergo an additional reaction to yield a more reduced product rather than elimination of a D or H to restore the original π-system.

The rate constant for radiation-induced D-to-H exchange is far more temperature dependent in ethane than in benzene with a doubling of the rate constant when going from 20 to 50 K for the former and an increase of only about ~20% for the latter. These data are also consistent with differences in the proposed mechanisms. In the case of a reaction mechanism requiring the initial abstraction of a proton from the organic by the reactive species generated in the ice, an increase in temperature would provide additional energy to overcome any initial reaction barrier and would be expected to play a significant role in the observed reaction rate constant. In contrast, an increase in temperature is far less important for a mechanism in which electrophilic reactive species directly react with the π-system in benzene. In all experiments, increasing the temperature may slightly increase the mobility of ions and radicals within the ice, contributing to increased rate constants.

These data strongly suggest that the rate constants associated with radiation-induced D-to-H exchange for organic molecules embedded in water ice are highly dependent on the type of molecule being studied. These data demonstrate that these rate constants are an order of magnitude smaller for small aliphatic compounds than they are for larger aromatic compounds. Additionally, the ratios of k_1 to k_2 for benzene indicate that D-to-H exchange accounts for the vast majority of radiation driven chemistry in benzene. Consequently, aromatic compounds that are embedded in water ice will have their deuterium enrichments rapidly depleted relative to any aliphatic organic compounds that may be present in the same ice.

As stated in our previous paper (Qasim et al. 2022), there are caveats to directly applying these rate constants to chemical modeling. First, these experiments use two-component ices, which simplifies the potential chemistry. Second (as previously stated), the D/H exchange rate constants depend on the degree of deuteration in the reactant. Caveats aside, the results of these experiments suggest additional complications for attempts to use D/H ratios to determine the origins of individual molecules in extraterrestrial samples. Specifically, the data suggest that despite possessing similar initial deuterium enrichments, chemically dissimilar molecules may experience dramatically different levels of D-to-H exchange if exposed to radiation in water ice. These results suggest that additional care may be needed to account for this effect when comparing different compounds identified in extraterrestrial samples.

5. Conclusion

The rate constants k_1 for radiation-induced D-to-H exchange were demonstrated to increase with temperature from 20 to 50 K for C_2D_6 in H_2O and likewise from 20 to 100 K for C_6D_6 in H_2O. The rate k_1 constant nearly doubles for C_2D_6 in H_2O if the radiolysis is conducted at 50 K rather than 20 K, which is in notable contrast to the modest 20% increase for k_1 over the same temperature interval for C_6D_6 in H_2O. For C_2D_6 in H_2O, $k_2 > k_1$ indicating that the radiolysis process is more likely to generate a greater abundance of products other than C_2D_5H. In contrast, for C_6D_6 in H_2O, $k_1 \gg k_2$ indicating that C_6D_5H was overwhelmingly favored as a radiolysis product. Additionally, the k_1 for C_6D_6 in H_2O is an order of magnitude larger than k_1 for C_2D_6 in H_2O. The difference in rate constants is likely due to a combination of the ease with which H^{+} and $H^{\cdot}$ to react with the π-system in benzene's aromatic ring and the stability of the resulting intermediate species. The results of this work suggest that radiation will influence D-to-H exchange between organic compounds and water ice matrices. Notably, this could lead to different levels of deuterium exchange in organic compounds based on their molecular type, complicating attempts to use D/H ratios to identify the origins of these compounds. Since this depletion will be radiation dose dependent, these results also suggest that it will be most pronounced in ices that receive the largest radiation dose and should be attenuated for ices with lower exposure (e.g., ices at a greater depth from the surface of a large icy body). The findings of this work suggest that the radiation history of a sample plays a significant role in the D/H ratios of the organic compounds embedded in water ice. This issue could be relevant to the interpretation of D/H ratios in extraterrestrial samples analyzed in situ, acquired by sample return, or naturally delivered to Earth (e.g., meteorites).

This work was supported by the Solar System Workings program, award No. 18-SSW18-0027. Thank you to Reggie Hudson and Perry Gerakines for insightful discussions and for helping to shape the manuscript. Special thanks to Stephen Brown and Eugene Gerashchenko for maintenance and

operation of the Van de Graaff accelerator in the Radiation Effects Facility at GSFC.

ORCID iDs

Christopher K. Materese https://orcid.org/0000-0003-2146-4288

References

Benedict, W. S., Morikawa, K., Barnes, R. B., & Taylor, H. S. 1937, JChPh, 5, 1
Cleeves, L. I., Bergin, E. A., Alexander, C. M. O., et al. 2016, ApJ, 819, 13
Dalgarno, A., & Lepp, S. 1984, ApJL, 287, L47
Faure, A., Faure, M., Thulé, P., Quirico, E., & Schmitt, B 2015, A&A, 584, A98
Geiss, J., & Reeves, H. 1981, A&A, 93, 189
Hama, T., Ueta, H., Kouchi, A., & Watanabe, N. 2015, PNAS, 112, 7438
Herbst, E. 1982, A&A, 111, 76
Hiraoka, K., Takayama, T., Euchi, A., Handa, H., & Sato, T. 2000, ApJ, 532, 1029
Hudson, R. L., & Ferrante, R. F. 2020, MNRAS, 492, 283
Hudson, R. L., & Yarnall, Y. Y. 2022, Icar, 377, 114899
Kerridge, J. F., & Chang, S. 1985, in Protostars and Planets II, ed. D. C. Black & M. S. Matthews (Tucson, AZ: Univ. Arizona Press), 738
Kobayashi, H., Hidaka, H., Lamberts, T., et al. 2017, ApJ, 837, 155
Krishnamurthy, R. V., Epstein, S., Cronin, J. R., Pizzarello, S., & Yuen, G. U. 1992, GeCoA, 56, 4045
Lamberts, T., Fedoseev, G., Kästner, J., Ioppolo, S., & Linnartz, H. 2017, A&A, 599, A132
Moore, M. H., Hudson, R. L., & Gerakines, P. A. 2001, AcSpA, 57, 843
Nanney, T. R., Lippincott, E. R., & Hamer, J. C. 1966, AcSpe, 22, 737
Paranicas, C., Cooper, J. F., Garrett, H. B., Johnson, R. E., & Sturner, S. J. 2009, in Europa, ed. R. T. Pappalardo, W. B. McKinnon, & K. K. Khurana (Tucson, AZ: Univ. Arizona Press), 529
Pinchas, S., & Laulicht, I. 1971, Infrared Spectra of Labelled Compounds (New York, NY: Academic Press), 74
Qasim, D., Hudson, R. L., & Materese, C. K. 2022, ApJ, 929, 176
Robert, F., & Epstein, S. 1982, GeCoA, 46, 81
Sandford, S. A., Bernstein, M. P., Allamandola, L. J., Gillette, J. S., & Zare, R. N. 2000, ApJ, 538, 691
Sandford, S. A., Bernstein, M. P., & Dworkin, J. P. 2001, M&PS, 36, 1117
Satorre, M., Millán, C., Molpeceres, G., et al. 2017, Icar, 296, 179
Smith, D., Adams, N. G., & Alge, E. 1982, ApJ, 263, 123
Snyder, L. E., Hollis, J. M., Buhl, D., & Watson, W. D. 1977, ApJL, 218, L61
Stitt, F. J. 1939, ChPhy, 7, 297
Strazzulla, G., Cooper, J. F., Christian, E. R., & Johnson, R. E. 2003, CRPhy, 4, 791
Tielens, A. G. G. M. 1983, A&A, 119, 177
Watanabe, N., & Kouchi, A. 2008, PrSS, 83, 439
Watson, W. D. 1976, RvMP, 48, 513
Watson, W. D. 1977, Acc. Chem. Res., 10, 221
Yang, J., & Epstein, S. I. 1983, GeCoA, 47, 2199
Ziegler, J. F., Ziegler, M. D., & Biersack, J. P. 2010, NIMPB, 268, 1818